T. FERNHOLZ
H. TEICHERT
V. EBERT✉

Digital, phase-sensitive detection for *in situ* diode-laser spectroscopy under rapidly changing transmission conditions

Universität Heidelberg, Physikalisch-Chemisches Institut, Im Neuenheimer Feld 253, 69120 Heidelberg, Germany

ABSTRACT A new harmonic detection scheme for fully **d**igital, **f**ast-**s**canning **w**avelength-**m**odulation **s**pectroscopy (DFS-WMS) is presented. DFS-WMS is specially suited for *in situ* absorption measurements in combustion environments under fast fluctuating transmission conditions and is demonstrated for the first time by open-path monitoring of ambient oxygen using a distributed-feedback diode laser, which is doubly modulated with a fast linear 1 kHz-scan and a sinusoidal 300 kHz-modulation. After an analog high-pass filter, the detector signal is digitized with a 5 megasample/s 12-bit AD-converter card plugged into a PC and subsequently – unlike standard lock-ins – filtered further by co-adding 100 scans, to generate a narrowband comb filter. All further filtering and the demodulation are performed completely digitally on a PC with the help of discrete Fourier transforms (DFT). Both $1f$- and $2f$-signals, are simultaneously extracted from the detector signal using one ADC input channel. For the $2f$-signal, a linearity of 2% and a minimum detectable absorption of 10^{-4} could be verified experimentally, with the sensitivity to date being limited only by insufficient gain on the $2f$-frequency channel. Using the offset in the $1f$ signal as a transmission 'probe', we could show that the $2f$-signal can be transmission-corrected by a simple division by the $1f$-background, proving that DFS-WMS provides the possibility of compensating for transmission fluctuations. With the inherent suppression of additive noise, DFS-WMS seems well suited for quantitative *in situ* absorption spectroscopy in large combustion systems. This assumption is supported by the first measurements of oxygen in a high-pressure combustor at 12 bar.

PACS 39.30+w; 42.62.F; 42.62.Lf; 42.55.Px; 42.30.L; 42.60.Fc

1   Introduction

High-resolution laser absorption spectroscopy (LAS) is a well-known and robust diagnostic technique, which is capable of providing species information with high sensitivity, speed and selectivity. The advantages of this technique have been demonstrated frequently in laboratory environments. However, an affordable scale-up of such laser-based gas sensors to accommodate *in situ* measurements in

✉ Fax: +49-6221/545-050, E-mail:volker.ebert@pci.uni-heidelberg.de

'real-world' processes is hampered by many problems which have to be solved in order to realize a widespread technical application, e.g. for active combustion control and optimization.

First of all, there is a need for a suitable laser source. This problem can be solved by the use of near-infrared diode lasers (NIR-DLs), which were initially developed for communication applications, and which have shown rapid improvement over the last decade. In comparison to alternative laser sources, NIR-DLs offer a rather unique combination of excellent spectroscopic and technical properties. These are: narrow linewidth for high spectral resolution, relatively high optical cw output power – compared to MIR lasers – which can compensate for severe losses in *in situ* measurements, and excellent tunability, allowing efficient noise reduction techniques. The excellent technical properties are: room-temperature operation, high wall plug efficiency, long life time, compactness, compatibility with low-cost room-temperature detectors and glass fibers and finally a rather low price.

Optical *in situ* sensors based on LAS offer many advantages (higher speed, no corrosion, no point measurement) over extractive techniques, avoiding errors like adsorption, condensation, chemical reaction and fractionation, which are related to the gas sampling process. In contrast, it is much more demanding to quantitatively evaluate a heavily disturbed and weak *in situ* absorption signal, that is sometimes up to two or three orders of magnitude weaker than competing disturbances, e.g. fast broadband transmission variations of the measurement path or background radiation in the case of luminous (combustion) processes.

Over the last few years, we have developed various spectrometers based on direct tunable-diode-laser absorption spectroscopy (direct TDLAS) and have realized simultaneous species and temperature measurements in full-scale power plants (incinerators, gas-fired and coal-fired power plants). Up to four species (O_2, CH_4, H_2O, CO_2) have been detected by probing the same volume with a composite laser beam [1–5]. Even under the very low transmission conditions (total light losses of 99.99%) found in coal-fired power plants, measurements of water and CO concentrations and gas temperatures could be realized [1, 4]. The basic principle of measurement is described in detail elsewhere [2, 5–7]. This takes advantage of the versatile tuning capabilities of diode lasers (slow coarse tuning by temperature and fast fine tuning by current variation). Complete profiles of the absorption line are

captured by rapidly scanning the laser wavelength with a linear current ramp over a suitable spectral interval. The laser power transmitted through the measurement volume – governed by an extended Beer's law [1, 2] – is detected directly with a dc-coupled, optically filtered photodetector and digitized by a fast AD-converter. By scanning the laser much faster (multi kHz) than the typical transmission or emission fluctuations we ensured these effects were constant during the scan. Additive contributions to the detected signal are then determined and removed by turning the laser off for a short period of time during the scan or by using the characterized amplitude modulation (AM) of the laser [4]. In contrast, multiplicative transmission fluctuations are extracted from the baseline of the scan (the baseline being the transmitted laser power in the absence of a molecular absorption) by fitting an absorption line model (e.g. Voigt or Lorentzian [8]) and a low-order background polynomial to the offset corrected scan data [2, 5]. By knowing the gas temperature, pressure, absorption path length and spectroscopic data of the laser and of the absorption line under investigation, we can – without any calibration – convert the line area determined by the fitting routine to an absolute absorber number density. With these spectrometers, we achieved typical minimum detectable absorptions (MDAs) of the order of 10^{-3} to 10^{-4} optical density (OD) at a response time of a few seconds using standard 12-bit AD converters [2, 5].

Much better MDAs, up to 10^{-8}, and even close to the theoretical shot noise limit for an absorption measurement [9, 10] have been reported for other modulation schemes involving dual-beam subtraction (DBS) [11, 12] or the very common dual-frequency modulation/harmonic detection techniques [termed wavelength-modulation spectroscopy (WMS), frequency-modulation spectroscopy (FMS), single-tone (ST) and two-tone (TT) FMS] [13–15]. All these techniques reject the large offset in the DC-coupled transmission signal – thereby losing their transmission and emission information – to guarantee much better use of the dynamics of the electronic system. This is done by severe additional narrowband filtering using lock-in amplifiers or scan averaging. However, these techniques are mostly limited to conditions with no or only mild transmission disturbances.

As most of these detection schemes are based on standard lock-in amplifiers, they cannot be used in environments with strong transmission variations, since single-channel harmonic-detection strategies can only suppress additive noise. Multiplicative noise, e.g. transmission noise, on the input signal has to be accounted for by simultaneous determination using a second independent measurement (e.g. two spectral channels) in order to distinguish between changes in the broadband absorption (transmissivity) and specific absorption.

Such a transmission-corrected dual-channel WMS technique was reported by us recently [16] and was successfully applied to an *in situ* measurement of oxygen in a full-scale waste incinerator. However, limitations were expected for faster and stronger transmission fluctuations due to the low scan frequency of 9 Hz.

In this paper, we present a new fast-scanning transmission-corrected WMS (DFS-WMS) approach suitable for *in situ* applications. It is based on a fast 12-bit AD converter plug-in board and a PC. DFS-WMS completely avoids slow standard analog lock-in amplifiers, and offers scanning frequencies in the multi-kHz range. All mathematical operations are performed on a PC. We present results of the first experiments for the detection of oxygen and tests on the linearity and sensitivity.

2 Measurement principles

2.1 *Harmonic detection*

The basic principle of harmonic detection takes advantage of the fact that a sinusoidal modulation of the argument of a non-linear transfer function produces an output signal that contains higher harmonics of the fundamental frequency. If the argument is complex, these harmonics will be proportional to the derivatives of the transfer function. For real arguments, this will remain valid if the modulation amplitude is small and a first-order approximation can be applied. The output signal can be calculated using the Taylor series of the transfer function. The real modulation can be expressed by two complex terms with positive and negative frequencies, which produce cross terms given by the binomial formula:

$$g(v + A\cos\omega t) = g\left(v + \frac{A}{2}\left(e^{i\omega t} + e^{-i\omega t}\right)\right)$$
$$= \sum_{n=0}^{\infty} \frac{1}{n!} g^{(n)}(v) \left(\frac{A}{2}\right)^n \sum_{j=0}^{n} \binom{n}{j} e^{i(n-2j)\omega t}.$$
(1)

Here $g^{(n)}(v)$ denotes the transfer function and its derivatives of nth order, v is the mean value of the argument and A and ω describe the modulation amplitude and frequency, respectively.

The summation can easily be rearranged with respect to different harmonics:

$$g(v + A\cos\omega t) = \sum_{n=0}^{\infty} H_n(A, v) \cos n\omega t,$$
(2)

$$H_n(A, v) = \sum_{j=0}^{\infty} \frac{\varepsilon_n}{j!(n+j)!} \left(\frac{A}{2}\right)^{n+2j} g^{(n+2j)}(v)$$
(3)

$$\varepsilon_n = \begin{cases} 1; & n = 0 \\ 2; & n = 1, 2, 3, \ldots \end{cases}.$$

It is more complicated to give an analytical expression for a certain transfer function. The amplitudes of the harmonic components for a normalized Lorentzian line profile were given by Arndt [17]:

$$H_n(m, x) = \frac{\varepsilon_n}{2} \frac{i^n}{m^n} \cdot \frac{\left[\sqrt{(1-ix)^2 + m^2} - (1-ix)\right]^n}{\sqrt{(1-ix)^2 + m^2}} + c.c.$$
(4)

$$m = \frac{A}{\gamma} \qquad x = \frac{v}{\gamma} \qquad \varepsilon_n = \begin{cases} 1; & n = 0 \\ 2; & n = 1, 2, 3, \ldots \end{cases}. \quad (5)$$

Here, the modulation depth A and the center frequency v are scaled by the linewidth γ and the line center is chosen to be zero. Also, c.c. means conjugated complex.

2.2   Diode-laser modulation

In diode-laser spectroscopy, the transfer function is basically given by the molecular absorption of the sample, with the argument being the wavelength of the probing laser. The laser is usually driven with a doubly modulated injection current. A slow modulation (termed *scan*) varies the center wavelength of the laser at a repetition rate f while the harmonics of a fast sinusoidal modulation (frequency ω) can be detected with varying amplitude in the presence of an absorption feature. The laser current modulation leads to a variation in the laser output power as well as in the laser wavelength. One should note that the wavelength modulation exhibits a strong dependence on the modulation frequency and produces a phase shift, while the variation of the output power can be treated as following the injection current instantaneously. See [18–22] for a detailed description. If additive noise is neglected, the detected signal can be factorized to three terms for the laser output power P, the transfer characteristic g, including the molecular absorption feature, and the broadband transmissivity T of the sample:

$$P_{\mathrm{det}}(t) = P\left(I(t)\right) \times g\left(v(t)\right) \times T(t),\tag{6}$$

$$I(t) = I_{\mathrm{scan}}(t) + \hat{I}\cos\omega t,\tag{7}$$

$$v(t) = v_{\mathrm{scan}}(t) + k_v\hat{I}\cos(\omega t - \varphi).\tag{8}$$

$\hat{I}$ is the amplitude of the fast current modulation, k_v denotes the dynamic tuning coefficient of the laser wavelength (or frequency) v and φ is the phase shift between current and wavelength modulation, which should range between $0°$ and $90°$ for purely relaxational processes.

The dependence of the output power on the injection current can usually be assumed to be linear with a slope k_p. If the transmissivity is constant or corrected, the detected signal follows from (2):

$$\frac{P_{\mathrm{det}}(t)}{T(t)} = \left(P_{\mathrm{scan}}(t) + k_p\hat{I}\cos\omega t\right)\tag{9}$$

$$\times \sum_{n=0}^{\infty} H_n\left(k_v\hat{I}, v_{\mathrm{scan}}(t)\right)\cos n(\omega t - \varphi).$$

The amplitude modulation leads to a superposition of neighboring harmonic terms because the mixing product contains the sum and difference frequencies. Therefore, each harmonic channel contains not only the corresponding H_n-term but also contributions from its successor and its predecessor. Arranging the terms accordingly leads to the following summation. The terms for the first two channels, i.e. the 0ω- and 1ω-signals, require special treatment, because there are no negative frequencies in real signals.

$$\frac{P_{\mathrm{det}}(t)}{T(t)} = P_{\mathrm{scan}}(t) \times H_{\mathrm{scan}}^0(t) + \frac{k_p\hat{I}}{2} \times H_{\mathrm{scan}}^1(t)\cos(\varphi)$$

$$+ \sum_{n=1}^{\infty} P_{\mathrm{scan}}(t) \times H_{\mathrm{scan}}^n(t)\cos(n(\omega t - \varphi))$$

$$+ \frac{k_p\hat{I}}{2} \sum_{n=1}^{\infty} \varepsilon_n' H_{\mathrm{scan}}^{n-1}(t)\cos(n(\omega t - \varphi) + \varphi)$$

$$+ \frac{k_p\hat{I}}{2} \sum_{n=1}^{\infty} H_{\mathrm{scan}}^{n+1}(t)\cos(n(\omega t - \varphi) - \varphi),\tag{10}$$

$$H_{\mathrm{scan}}^n(t) = H_n\left(k_v\hat{I}, v_{\mathrm{scan}}(t)\right)\tag{11}$$

$$\varepsilon_n' = \begin{cases} 2; & n = 1 \\ 1; & n = 2, 3, 4, \dots \end{cases}.\tag{12}$$

In this description, we completely neglect effects that can be introduced by non-linear characteristics of the diode laser or optical components. These background signals have been analyzed in detail by Axner and Kluczynski [23–25].

2.3   Spectral representation

If both current modulations are periodic and the transmissivity is constant, the spectrum of the detected signal will be discrete. Its principal structure is shown in Fig. 1. The periodic scan of the center wavelength at frequency f produces sidebands $\pm m \times f$ at each harmonic frequency $n \times \omega$ of the fast modulation. These sidebands contain the information on the varying amplitudes of the spectral components during the scan, reflecting the amplitude modulation of the laser and the non-linearity of the transfer function. If a lock-in amplifier is used to extract a harmonic channel $n \times \omega$, its bandwidth must cover the complete sideband of the specific channel. Otherwise, the absorption feature will be distorted or suppressed. Accordingly, it is necessary to keep the scan frequency very low in order to achieve a high signal-to-noise ratio by using a narrow detection bandwidth, i.e., a long lock-in integration time.
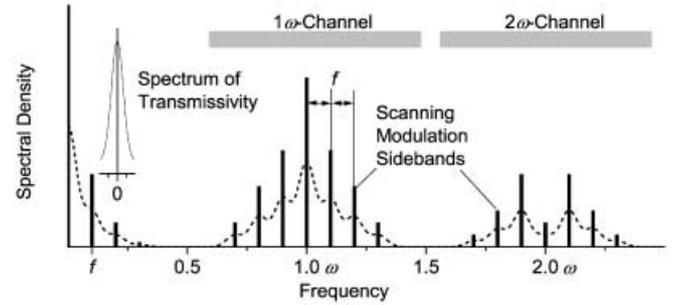

FIGURE 1   Schematic diagram for the spectral representation of the detected signal. If the transmissivity is fluctuating, the spectrum will be given by a convolution of the frequency characteristics of the fluctuations (*inset*) and the unperturbed discrete spectrum. See text for details

2.4   Fast fluctuating transmissivity

If the transmissivity of the optical path fluctuates during the measurement, the complete spectrum of the detector signal will be given by a convolution of the discrete frequencies with the frequency characteristics of the transmission noise. This is due to the multiplicative character of the transmission disturbances. If the scan frequency is low compared to the transmission fluctuations, the continuous side-

bands, which are due to the varying transmissivity, will overlap and completely cover the unperturbed signal.

Recently, we reported experiments in which we simultaneously recorded two harmonic channels using two standard lock-in amplifiers. The instant transmissivity was extracted from the background in the amplitude of the first harmonic (1ω-signal) [16]. The major contribution to the 1ω-signal is generated by the inherent amplitude modulation (AM) of the laser when modulating the current. If contributions of molecular absorption features to the 1ω-signal can be separated, the spectrum can be deconvoluted by dividing the 2ω-signal by the 1ω-background in the time domain, thereby using the laser AM as a transmission 'probe'. The separation was achieved by a least-squares fit to the 1ω-signal with a model that includes the specific absorption features and a slowly varying background. However, this approach will only be feasible if the transmission-related fluctuations are small enough so that the absorption feature can be separated clearly from the background, and if their frequency characteristics are totally different from those of the scan.

In direct absorption spectroscopy (baseband detection) the absorption signal can be recovered from the disturbed signal when a relatively fast scan frequency (f) in the kilohertz range is used. The harmonics of the scan frequency spread and the overlap of the continuous transmissivity sidebands will be minimized. Typically, the signal will be digitized and synchronously averaged over a certain number of scan periods. In the frequency domain, this can be described by applying a comb filter to the signal. The free spectral range of the filter is given by the scan frequency while its bandwidth is limited by the length of the averaging time interval. In the ideal case of non-overlapping transmission sidebands and infinitely small bandwidth, the recovered signal differs from the unperturbed signal only by a constant factor and a constant offset, which represent the mean transmissivity and the mean background signal. The signal can then be evaluated by means of a least-squares fit [1–4].

Here, we apply the same principle to the harmonic detection scheme. The discrete sidebands $\pm m \times f$ of each harmonic channel $n \times \omega$ spread widely when a scan frequency f in the kilohertz range is used. Instead of filtering the harmonic channel with a RC-filter we reduce the bandwidth of the detected signal by applying a comb filter. This is done by digitizing the doubly modulated signal and synchronously averaging it over several scans. All components of the signal which are not periodic with the scan rate will be averaged out. The origin of the equivalent comb filter is always at frequency zero. Hence, the fast modulation frequency ω must be an exact multiple of the scan frequency f to match the position of the harmonic channels, the scanning frequency side bands and the notches of the comb filter. The phase-sensitive demodulation of the signal is performed by the following procedure: A discrete Fourier transform (DFT) yields the spectral representation of the signal. The complete amplitude and phase information could be obtained using sine and cosine transforms. It is mathematically equivalent to perform a complex transform ignoring the negative frequency components. A single harmonic channel, i.e. a frequency window of limited width centered on a harmonic frequency $n \times \omega$, is separated by digitally filtering it. This could also be done electronically before digitizing the signal. The demodulation itself is done by transforming the signal back to the time domain after shifting the spectrum such that the center frequency of the selected harmonic channel becomes zero. This has the same effect as dividing the complex signal in the time domain by a complex harmonic function whose frequency is given by the center frequency of the desired channel.

The result of the whole operation gives the time evolution of the amplitude and phase of the respective channel. As in the case of direct absorption spectroscopy, the ideally recovered signal differs from the unperturbed signal only by a constant factor which represents the mean transmissivity.

The digital procedure is equivalent to mixing the signal with a local oscillator and demodulating it, as is used for heterodyne detection in a common FM-radio. One could of course perform analog mixing before digitizing the signal. However, if the detected signal is transformed down to frequency zero, only one phase component can be recorded on one digital channel. This is because with real signals the images of the positive and negative frequency components will recombine.

2.5 *Signal recovery*

By using the scheme presented above, the fluctuations of transmissivity can be corrected as already mentioned. A least-squares fit to the 1ω-signal can be used to extract the instant transmissivity, which gives the correction factor for any other harmonic channel.

The fitting procedure will become obsolete, if the scan covers the absorption feature completely, if the distortion of the signal due to the varying laser output power can be neglected and if the absorption is small (a few percent). In this case, the 1ω-signal will be almost symmetric with respect to its mean value, which will be proportional to the transmissivity. Since the scan frequency in this case is much higher than in our earlier experiments [16], the transmissivity can be assumed to be constant over the scan and hence a much better transmission correction can be achieved.

3 Experimental

A simple experiment demonstrates the principle of operation under laboratory conditions and allows us to derive values for the quality of the signals that can be expected under *in situ* conditions.

3.1 *Set-up*

The experimental set-up is shown in Fig. 2. A distributed-feedback diode laser (Sensors Unlimited, DFB-SU2054) was used to detect a single absorption line of oxygen in air at a wavelength of $\lambda_{\text{vac}} = 761$ nm, $b^1 \Sigma_g^+ \leftarrow X^3 \Sigma_g^-$ transition, ($v = 0 \leftarrow v = 0$) *A* band, R7R7 [26]. The absorption length was varied between 30 and 70 cm, which led to a maximum peak absorption of 1.5%. The Peltier-cooled laser was powered and modulated via a combined diode-laser driver/temperature controller (Melles Griot, 06DLD103). Two function generators (Stanford Research Systems, DS345) supplied a triangular scanning modulation (1 kHz) and a sinusoidal modulation (300 kHz), which were added using
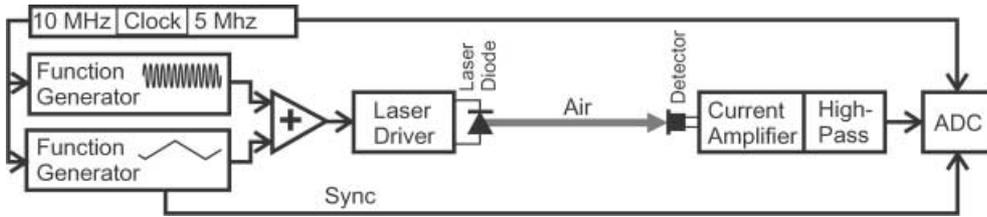
FIGURE 2   Experimental set-up: A diode laser beam is directed onto a photodetector through ambient air with varying absorption path length. The laser is driven with a doubly modulated injection current. The amplified, high-pass filtered signal is recorded using an analog-to-digital converter board (ADC). A double frequency clock is used to synchronize the two function generators and the A/D converter

a voltage amplifier (Stanford Research Systems, SR560). The signal from a biased photodiode (silicon, $\varnothing$3 mm, 5 V) was high-pass filtered (10 kHz) and amplified by a low-noise current pre-amplifier (3-dB-bandwidth 500 kHz, Stanford Research Systems, SR570). A personal computer with a fast AD-converter plug-in card (National Instruments, 6110E, 5 megasamples/s) was used to record the signal and to perform the calculations. A third function generator (SRS, DS345) provided 10 and 5 MHz clocks for the modulation and the data acquisition in order to achieve full timing control.

3.2   *Timing*

Proper timing and synchronization is crucial for the given set-up as we perform phase-locked scan averaging. If the modulation frequency ω is not an exact multiple of the scan frequency f or if there is jitter, the comb filter will not cover the modulation frequency, its harmonics and all their sidebands, i.e. most of the arising frequencies will be averaged out.

Since a discrete Fourier transform (DFT) is used in the calculations, it is important to sample an integer number of modulation periods. This is because a periodic input signal is assumed for the DFT-algorithm. In other words, the algorithm expands the input signal into a linear superposition of orthonormal sine and cosine functions that are periodic with the sampling interval. If the algorithm is fed with a fractional number of modulation periods, the modulation frequency and its harmonics will not be projected onto δ-functions and the harmonic channels cannot be separated clearly. This requirement will be fulfilled for all arising frequencies, including the sidebands, only if complete scanning periods are sampled and if the sampling frequency is again an exact multiple of the scan frequency. If it is desired to use the scan period only partially, the sampling rate of the ADC should be chosen to be an integer multiple of the modulation frequency. This allows for the sampling of an arbitrary but integer number of modulation periods.

4   Results

In Fig. 3, the result of a discrete Fourier transform of the input signal sampled at 5 megasamples/s is presented. The signal was averaged over 100 scan periods equivalent to an integration time of 100 ms. We want to emphasize that the comb structure of the equivalent analog signal is lost in the digital spectrum because only integer multiples of the scan frequency are represented. The same effective channel bandwidth could have been achieved with an analog lock-in amplifier only with a low scan frequency of 10 Hz. The analog sig-
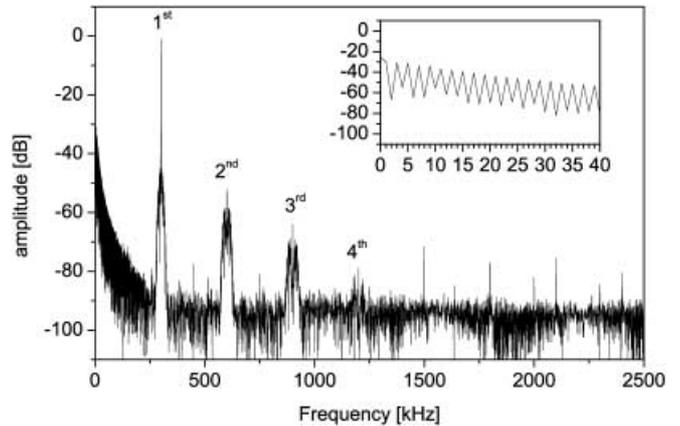

FIGURE 3   Logarithmic plot of the amplitude spectrum of the recorded signal. The *inset* shows the low-frequency part of the spectrum. See text for details

nal was high-pass filtered with a cut-off frequency of 10 kHz, which suppressed most of the triangular amplitude modulation caused by the scanning (0ω-signal). The inset shows the low-frequency part of the spectrum, which produces significant amplitudes at odd multiples of the scan frequency due to the symmetric character of the scan. The spectrum clearly shows four harmonics of the modulation frequency ($n \times \omega$). Each harmonic channel is spread over roughly 100 kHz. The fundamental channel (1ω) produces a strong carrier, which results from the inherent amplitude modulation of the laser output power. The noise level is -90 dB, compared to a maximum signal amplitude of 1 V, which perfectly reflects the theoretical value of -92 dB when averaging over 100 scan periods at an A/D resolution of 12 bit [28].

The demodulated signals of the first two channels (1ω and 2ω) are shown in Figs. 4 and 5. The modulation depth was chosen such that the relative 2ω-signal was maximized (2ω-to-1ω-ratio). According to (10), three terms with different phases contribute to each of the signals. Here, we neglect the H_{n+1}-contributions because for small modulation depths and a narrow scan width they should be weak compared to the other terms. We use the phase-plot of the 1ω-signal to approximately determine the phase shift between amplitude and frequency modulation of the diode laser. The overall phase introduced by the electronics [27] is taken from the mean value of the signal, which is almost only dependent on the H_0-contribution for the following reasons: The scan covers the absorption line completely and symmetry will lead to a vanishing mean value of the H_2-term if no further non-linearity is present and if the frequency scanning can be assumed to be linear. In contrast, the H_1-term exhibits a slight asymme-
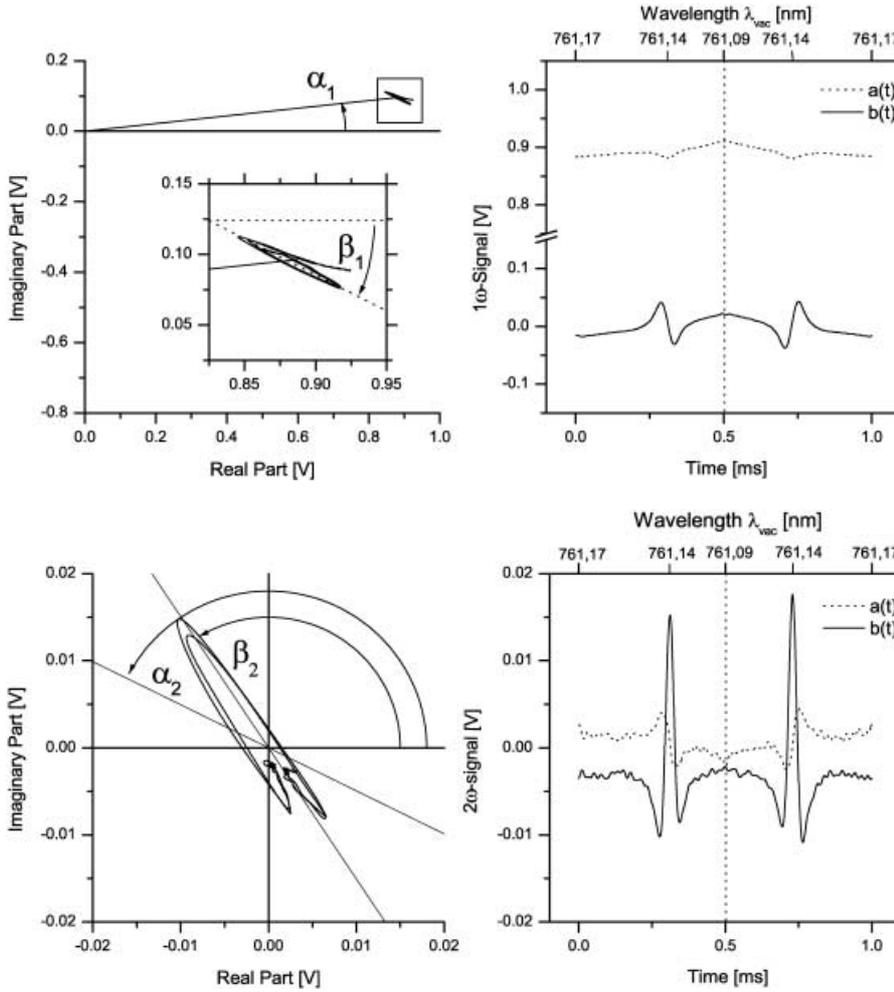
FIGURE 4 Recorded 1ω-signal: phase-plot (*left*) and time evolution of the two components (*right*). The angle α_1 denotes the overall phase shift. The phase shift φ between amplitude and frequency modulation is given by $\beta_1 - \alpha_1 = 33.1°$. The injection current was scanned with a triangular function and is lowest at the center of the scan. See text for details

FIGURE 5 Recorded 2ω-signal: phase plot (*left*) and time evolution of the two components (*right*). The angles α_2 and β_2 denote the absolute phases of the two contributing components. They differ by $\varphi = 33.1°$. The injection current was scanned with a triangular function and is lowest at the center of the scan. The timescale refers to a single scan period. See text for details

try due to the power modulation of the laser. However, this can be neglected because the linewidth is less than 10% of the scan width. After removing the mean value of the 1ω-signal and correcting for the overall phase, the major contribution to the remaining signal exhibits a rotation that is due to the phase shift of the frequency modulation ($\varphi = 33.1°$). In order to separate the signal contributions correctly, we apply the following transformation after taking the real and imaginary parts:

$$\begin{pmatrix} a(t) \\ b(t) \end{pmatrix} = \frac{1}{\sin(\beta_1 - \alpha_1)} \begin{pmatrix} \sin\beta_1 & -\cos\beta_1 \\ -\sin\alpha_1 & \cos\alpha_1 \end{pmatrix} \cdot \begin{pmatrix} \mathrm{Re}(t) \\ \mathrm{Im}(t) \end{pmatrix}. \tag{13}$$

The angles $\alpha_1 = 6.2°$ and $\beta_1 = -26.9°$ are given by the absolute phases of the amplitude and frequency modulations, respectively. The phase shift φ is given by the difference $\alpha_1 - \beta_1$.

The phases of the two major components of the 2ω-signal are identified by taking the difference between the signal at the line center (maximum modulus) and its mean value. The result yields the angle $\alpha_2 = 156.7°$. The angle β_2 is given by $\alpha_2 - \varphi = 123.6°$. In principle, the angle α_2 should equal β_1, but for the 2ω-signal the overall phase shift introduced by the electronics differs from that of the 1ω-signal. The mean value

of the signal is not zero because there is a slight overall nonlinearity in the output power modulation of the diode laser.

In both graphs, the $b(t)$-signals (H_n-contribution) slightly differ in amplitude on the two sides of the scan. This is due to the frequency dependence of the tuning coefficient of the laser, which also affects the low-frequency components. While the scanning of the injection current $I_{\mathrm{scan}}(t)$ is triangular, the frequency scanning $\nu_{\mathrm{scan}}(t)$ is not and always lags behind the output power modulation. The relative wavelength calibration was done by recording fringes produced by a 10-cm air-spaced Fabry–Perot-interferometer and a single triangular modulation of the laser at 1 kHz.

The procedure for correcting variations in transmissivity was checked by changing the length of the absorption path without proper beam alignment. At each position of the detector the laser was poorly adjusted to produce an arbitrary change in the amount of detected intensity. In Fig. 6, the magnitudes of the corrected and uncorrected 2ω-signals are plotted against the absorption path length. After correction, the dependence is perfectly linear, showing residuals of only 2%.

In principle, it should be possible to derive optical densities and absolute oxygen concentrations from the recorded data, if the characteristic coefficients of the diode laser are known. However, in contrast to direct TDLAS, an uncertainty in the actual width of the absorption feature introduces a large
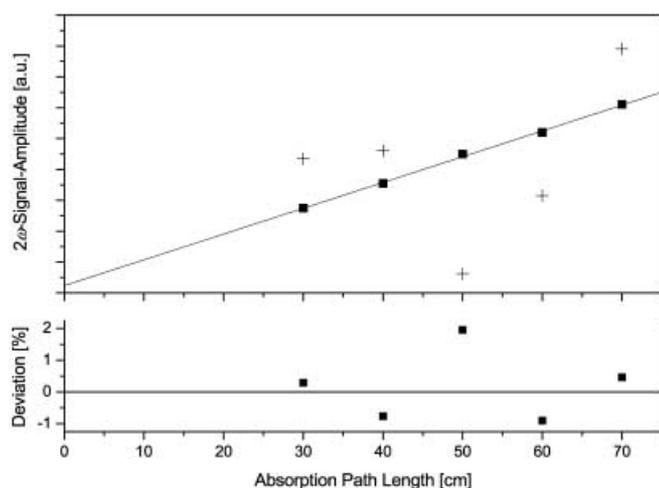
FIGURE 6   Test of linearity and noise of the presented fast-scanning digital lock-in scheme applied to the detection of oxygen in ambient air. In the *upper part* the magnitude of the 2ω-signals (maximum to mean shoulder) is plotted against the absorption path length under varying transmission of laser power. The graph shows uncorrected (*crosses*) and transmission-corrected (*squares*) data. The *lower part* shows the deviation of the corrected data from the fitted straight line

FIGURE 7   Second-harmonic signals from a strongly pressure-broadened oxygen absorption line detected in situ with a preliminary version of the new fast-scanning digital lock-in scheme in the flue gas duct of a 1 MW high-pressure coal combustor. Signals for different modulation depths are shown

error to the derived values as the signals strongly depend on the ratio of modulation depth to linewidth. Therefore, wavelength modulation spectroscopy will usually be calibrated with a known sample.

The absorption in this experiment was of the order of 10^{-2} optical density (OD). This can also be seen in the H_0-contribution to the 1ω-signal, which almost reflects the direct-absorption signal. With the accuracy given above, the minimum detectable absorption is 10^{-4} OD. With regard to the sensitivity, the same value can be derived from the signal-to-noise ratio in the recorded spectra (40 dB) [28]. However, it should be noted that the signal level of the 2ω-signal is -50 dB. It can be increased by using a second channel with a higher gain and an analog filter that suppresses the 1ω-signal.

From these data it can be expected that the relative accuracy under *in situ* conditions will be at least 2%, if the spectral components of the transmission noise stay below 1 kHz. With improved analog filtering and by detecting the 2ω-signal with a separate filter channel with higher gain, it should be possible to reach sensitivities in the 10^{-6} range.

5   Conclusions

A new harmonic detection scheme for fully digital fast-scanning wavelength-modulation spectroscopy (DFS-WMS), suitable for *in situ* absorption measurements, has been presented. The signals produced by DFS-WMS are mathematically fully equivalent to signals from related techniques that incorporate standard lock-in amplifiers. In contrast to standard techniques, DFS-WMS provides the possibility of compensating for fast transmission fluctuations. By co-adding the doubly modulated scans (a fast triangular scan and a faster sinusoidal modulation) a comb filter is generated, which provides the same narrow bandwidth filtering as the standard lock-in techniques, and the same fast scanning frequencies as direct TDLAS. The low-frequency contributions caused by
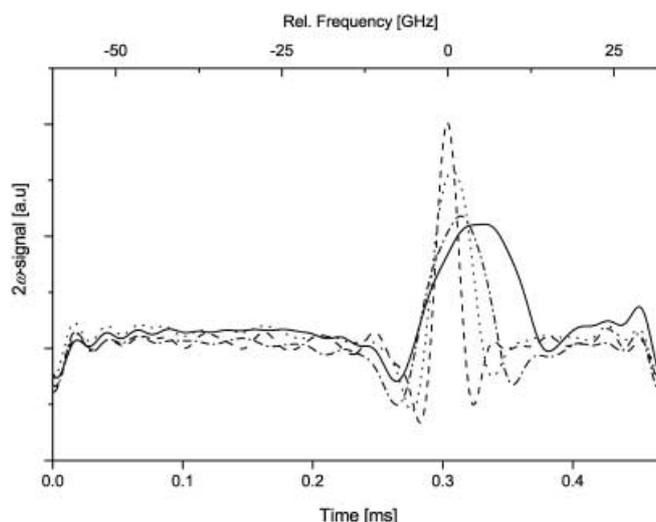
the transmission fluctuations are removed by using the large background in the 1ω-signal generated by the laser amplitude modulation as a transmission 'probe'. The transmission correction of the 2ω-signal is performed by a simple division by the 1ω-background. First measurements with slowly varying transmission have been presented and show that DFS-WMS is applicable. A sensitivity of 10^{-4} OD and a deviation from linearity of 2% was experimentally demonstrated by monitoring oxygen in air at 761 nm. A sensitivity of 10^{-6} OD seems to be feasible with a more dedicated electronics set-up.

At an earlier stage of our work, we also performed preliminary tests of DFS-WMS under *in situ* conditions. These tests were carried out at a high-pressure 1-MW coal combustion test facility using a vertical-cavity surface-emitting laser (VCSEL) at 770 nm (CSEM), which has also been used to monitor potassium concentrations [29]. We recorded second harmonic signals (2ω) of strongly pressure-broadened oxygen absorption lines at 12 bar in the flue gas duct approximately 2 m downstream from the combustion chamber. The laser light was subject to strong and fast transmission variations of transmissivity.

Figure 7 depicts several absorption profiles of an *in situ* O_2 line (P33Q32) for different amplitudes of fast ω-modulation. Due to the high scanning frequency, it was obviously possible to suppress all transmission fluctuations within the scan. However, the lack of proper synchronization between signal generation and A/D-conversion generated some modulating artifacts at the borders of the scans that spoiled the sensitivity. Further tests to determine the performance of DFS-WMS under 'real world' *in situ* conditions are underway.

REFERENCES

1 H. Teichert, T. Fernholz, V. Ebert: '*In Situ* Measurement of CO, H_2O and Gas Temperature in a Lignite-Fired Power-Plant'. In: *OSA Trends in Optics and Photonics (TOPS) Vol. 64, Laser Applications to Chemical and Environmental Analysis, OSA Technical Digest, Post-Conf. Edn.* (Optical Society of America, Washington DC 2002) pp. ThB3-1–ThB3-3

2 V. Ebert, T. Fernholz, C. Giesemann, H. Pitz, H. Teichert, J. Wolfrum, H. Jaritz: Proc. Combust. Inst. **28**, 423 (2000)

3 H. Pitz, T. Fernholz, C. Giesemann, V. Ebert: 'Diode-Laser-Based In-Situ CH_4-Detection for the Surveillance of Ignition Processes in Gas-fired Power-Plants'. In: *Laser Applications to Chemical and Environmental Analysis, OSA Technical Digest* (Optical Society of America, Washington DC 2000) pp. 111–113

4 T. Fernholz, H. Pitz, V. Ebert: '*In-Situ* Monitoring of Water Vapor and Gas Temperature in a Coal-Fired Power-Plant using Near-Infrared Diode Lasers'. In: *Laser Applications to Chemical and Environmental Analysis, OSA Technical Digest* (Optical Society of America, Washington DC 2000) pp. 77–79

5 V. Ebert, J. Fitzer, I. Gerstenberg, K.U. Pleban, H. Pitz, J. Wolfrum, M. Jochem, J. Martin: Proc. Combust. Inst. **27**, 1301 (1998)

6 D.E. Jennings: Appl. Opt. **19**, 2695 (1980)

7 D.T. Cassidy, J. Reid: Appl. Opt. **21**, 2527 (1982)

8 V. Ebert, J. Wolfrum: 'Absorption Spectroscopy'. In: *Optical Measurements – Techniques and Applications*, 2nd edn. ed. by F. Mayinger, O. Feldmann (Springer-Verlag, Heidelberg, München 2001) pp. 227–265

9 P. Werle, F. Slemr, M. Gehrtz, C. Bräuchle: Appl. Phys. B **49**, 99 (1989)

10 M. Gehrtz, G.C. Bjorklund, E.A. Witthaker: J. Opt. Soc. Am. B **2–9**, 1510 (1985)

11 P. Vogel, V. Ebert: Appl. Phys. B **72**, 127 (2001)

12 D.M. Sonnenfroh, M.G. Allen: Appl. Opt. **35**, 4053 (1996)

13 J.A. Silver: Appl. Opt. **31**, 707 (1992)

14 D.S. Bomse, J.A. Silver, A.C. Stanton: Appl. Opt. **31**, 718 (1992)

15 L. Wang, H. Riris, C.B. Carlisle, T.F. Gallagher: Appl. Opt. **27**, 2071 (1988)

16 V. Ebert, K.U. Pleban, J. Wolfrum: 'In-Situ Oxygen-Monitoring using Near-Infrared Diode Lasers and Wavelength Modulation Spectroscopy'. In: *Laser Applications to Chemical and Environmental Analysis, Technical Digest* (Optical Society of America, Washington DC 1998) pp. 206–209

17 R. Arndt: J. Appl. Opt. **36**, 2522 (1965)

18 K. Petermann: *Laser Diode Modulation and Noise* (Kluwer Academic Publishers, Dordrecht 1991)

19 S. Kobayashi, Y. Yamamoto, M. Ito, T. Kimura: IEEE J. Quantum Electron. **QE-18**, 582 (1982)

20 H.I. Abdelkader, H.H. Hausien, J.D. Martin: Rev. Sci. Instrum. **63**, 2004 (1992)

21 S. Kobayashi, Y. Yamamoto, M. Ito, T. Kimura: IEEE J. Quantum Electron. **QE-18**, 582 (1982)

22 M. Ito, T Kimura: IEEE J. Quantum Electron. **QE-17**, 787 (1981)

23 P. Kluczynski: Appl. Opt. **38**, 5803 (1999)

24 P. Kluczynski, M. Lindberg, O. Axner: Appl. Opt. **40**, 783 (2001)

25 P. Kluczynski, M. Lindberg, O. Axner: Appl. Opt. **40**, 794 (2001)

26 K.J. Ritter, T.D. Wilkerson: J. Mol. Spectrosc. **121**, 1 (1997)

27 Note: Here, the overall phase shift includes the phase shift between the two modulating function generators

28 Note: The levels refer to electrical power. When calculating optical ratios, the dB-values have to be divided by two as photodetectors convert optical power into voltage

29 E. Schlosser, T. Fernholz, H. Teichert, V. Ebert: Spectrochim. Acta **58**, 2347 (2002)